sustainability

MDPI

Article

Studying Thermal and Mechanical Properties of Recycled Concrete by Using Ceramic Aggregate

Yumei Wang [1,2], Jinyan Wang [3,4], Zhiheng Deng [4] and Jianzhuang Xiao [2,*]

[1] College of Architecture and Civil Engineering, Nanning University, Nanning 541699, China
[2] Department of Structural Engineering, College of Civil Engineering, Tongji University, Shanghai 200092, China
[3] College of Urban and Rural Construction, Guangxi Vocational University of Agriculture, Nanning 530007, China
[4] Guangxi Key Laboratory of Disaster Prevention and Engineering Safety, Guangxi University, Nanning 530004, China
* Correspondence: jzx@tongji.edu.cn

Abstract: Ceramic aggregate has the characteristics of light weight, heat insulation, and low cost, and recycled aggregate is a type of green material that realizes the re-crushing of construction waste. This paper studied the impact of replacing natural coarse aggregate with ceramic aggregate and natural sand with recycled fine aggregate, on the physical, mechanical, and thermal properties of concrete. Recycled fine aggregate was used to completely replace natural sand. A total of five concrete mixes (including a reference mix) were prepared with different levels of ceramic aggregate (0%, 30%, 50%, 70%, 100%). Density, compressive strength, thermal conductivity, and thermal inertia index were measured to evaluate the performance of each mixture, and ceramic concrete board and hollow blocks were designed for testing the thermal properties. Results of testing show that density, strength, and thermal performance are interrelated. The smaller the density, the lower the strength, and it indicates that ceramic aggregate has a negative influence on strength in concrete. Meanwhile, the smaller the density, the higher the thermal resistance, and the addition of ceramic aggregate can improve the thermal insulation of concrete. The mechanical and thermal properties are both affected by the ceramic replacement ratio. Ceramic aggregate improves the thermal properties of recycled concrete, and the negative influence of ceramic aggregate on compressive strength can be controlled by the replacement ratio of aggregate in concrete. Based on the overall comparison and analysis, a mix with 50% ceramic aggregate shows relatively better strength and thermal insulation compared to other mixes. The use of ceramic aggregate in combination with recycled fine aggregate can effectively reduce the environmental pollution and make an economical substitute for their natural counterparts.

Keywords: ceramic aggregate; recycled concrete; density; strength; thermal property

Citation: Wang, Y.; Wang, J.; Deng, Z.; Xiao, J. Studying Thermal and Mechanical Properties of Recycled Concrete by Using Ceramic Aggregate. *Sustainability* **2023**, *15*, 2642. https://doi.org/10.3390/su15032642

Academic Editors: Constantin Chalioris and Giouli Mihalakakou

Received: 24 October 2022
Revised: 7 January 2023
Accepted: 16 January 2023
Published: 1 February 2023

1. Introduction

Nowadays, energy has become the focus of all concern. Architecture energy consumption accounts for 30% of total society energy consumption [1], which is one of the burning issues of our times. Such a large slice of energy consumption has forced governments to make new proposals aimed at its reduction, whether in developed or developing countries [2,3]. For most developing countries, they also face the problem of over-exploitation of natural resources. A huge amount of solid waste has been produced, and more than 30% of the total solid waste is construction and demolition waste (CDW) [4–9]. For China, the world's largest CDW producer, the waste increases year by year, with the output of CDW being up to 2300 million tons in 2019 [6]. For the sustainable development of the construction industry, there is a compelling need to reduce the energy consumption and CDW generation [10,11].

The demand for environmental protection and energy conservation has made the appropriate design and construction of buildings with lightweight materials paramount [12–15]. The apparent density of lightweight concrete in the range of 800–1950 kg/m^3 can obviously reduce the dead load, while the use of ceramic concrete in buildings provides an environmental and economical structural solution [16–19]. Fan [20] conducted an experimental study to elevate curing temperature on ceramic concrete performance. This research intended to find an optimum mix proportion for ceramic concrete by orthogonal design. It investigated how the workability mechanical and thermal properties of lightweight aggregate concrete are related to each other, wanting to achieve the properties of low density with high thermal insulation [21]. Different particle sizes of ceramic aggregate were designed to study the insulation performance when being used as roof material in buildings [22], and the research reveals that using water storage bricks made from ceramic concrete in the energy-saving reconstruction of existing buildings roofs is feasible. Concrete made with ceramic aggregate has been proven a better thermal insulation product than conventional concrete due to its pore characteristics [23,24]. The impact of ceramic aggregate on the reliability of concrete considering performance of concrete based on strength has been broadly discussed [25–27]. Liu [28] found that the compressive strength, stability, and workability of the ceramic concrete were affected by the particle size of ceramic aggregate, and revealed that the compressive strength and workability of the ceramic concrete could be improved by the appropriate addition of mineral admixtures. Mineral admixtures and phase change materials have also been added in ceramic concrete to improve the mechanical and thermal properties [29–31].

Recycled aggregates are being promoted for use in concrete structures, because of their low cost and environmental friendliness [4,5,32,33]. The fine fraction of recycled aggregate absorbs more water due to its high porosity, which is imparted by the adhered mortar [34–36]. Most studies show that the mechanical properties of concrete decrease as the replacement ratio of fine recycled aggregate increases [37,38]. To improve the properties of recycled concrete, Etxeberria [39] proposed that both the quantity of recycled aggregates and production process have an impact on the performance of recycled aggregate concrete. Due to the shortage of natural sand, the use of recycled fine aggregate has become more important in concrete production. Evangelista and de Brito [38] demonstrate that the compressive strength is not affected by the utilization of recycled fine aggregate up to 30%, but Khatib [35] found that the compressive strength of concrete presents an obvious reduction with a high replacement ratio of recycled fine aggregate. The main effect on the behaviour of concrete with recycled fine aggregate is considered to be high porosity [40,41].

Concrete with a combination of ceramic pellets and recycled fine aggregates has not been explored well in the aspect of improving the thermal performance of concrete. The objective of this paper is to reveal the density, compressive strength, and thermal properties of concrete with fully replaced fine aggregates and increasing percentage of substitution of aggregate by ceramic, to eventually promote the application of environmentally friendly materials in construction.

2. Materials and Testing Procedure

Materials, Mixture and Test Procedure

(1) Materials

The ceramic particles used in this test were locally produced and made of industrial waste residue, mine tailing, fly ash, and other waste materials (Figure 1a). The ceramic was screened before use to obtain a good grading and the appropriate size of 5–10 mm was chosen. The material performance test was carried out according to "Lightweight aggregates and its test methods-Part 2: Test methods for lightweight aggregates" (GB/T 17431.2-2010 [42]; the physical properties of ceramic are shown in Table 1.

(**a**) (**b**)

Figure 1. Aggregate. (**a**) Ceramic aggregate. (**b**) Recycled fine aggregate.

Table 1. Physical properties of ceramic.

Gradation/mm	Apparent Density/kg/m^3	Crush Index/MPa	Water Absorption/1 h	Clay Content	Void Ratio
5–10	1231	6.3	11.3%	0.6%	39%

To study the influence of ceramic replacement ratio on concrete performance, natural crushed stone with a gradation of 5–10 mm was also used in the test. The material performance was tested based on "Pebble and crushed stone for construction" (GB/T 14685-2011) [43]; the physical properties of natural aggregate are shown in Table 2.

Table 2. Physical properties of natural aggregate.

Gradation /mm	Apparent Density /kg/m^3	Crush Index	Water Absorption /1 h	Clay Content	Void Ratio
5–10	2695	8.6%	0.3%	0.2%	32%

The recycled fine aggregate was from road waste concrete (Figure 1b). After the crushing, sieving, and washing process, the proper gradation of 0.16–5 mm as fine aggregate was chosen. The material test was carried out according to "Recycled fine aggregate for concrete and mortar" (GB/T 25176-2010) [44]. The recycled fine aggregate with fineness modulus of 2.9 has specific gravity 2.369; the physical properties are listed in Table 3. Ordinary tap water and P.O 32.5 Portland cement were used for mixing.

Table 3. Physical properties of recycled fine aggregate.

Gradation /mm	Apparent Density /kg/m^3	Crush Index	Water Absorption /1 h	Clay Content	Fineness Modulus
0.16~5	2369	21%	5.6%	1.2%	2.9

(2) Mixture

According to "Technical specification for lightweight aggregate concrete" (JGJ 51-2002) [45] and "Technical code on the application of recycled concrete" (DG/TJ08-2018-2007) [46], the amount of mixing water was selected according to the construction consistency requirements, the sand rate was selected according to the application of ceramic concrete, the total volume of ceramic aggregate and recycled sand was selected according to their types. The

amount of ceramic aggregate and recycled sand were calculated separately according to the following formula:

$$V_s = V_t \times S_p \quad (1)$$

$$m_s = V_s \times \rho_s \quad (2)$$

$$V_a = V_t - V_s \quad (3)$$

$$m_a = V_a \times \rho_a \quad (4)$$

In which V_s, V_a, and V_t represent the loose volume of fine aggregate, coarse aggregate, and total aggregate, respectively; m_s and m_a represent the weight of fine aggregate and coarse aggregate of 1 m^3. S_p represents the sand ratio, ρ_a and ρ_s represent the bulk density of coarse and fine aggregates, respectively.

The mix proportion was tentatively calculated, after repeating trials, the optimum water cement ratio (W/C) and sand ratio were determined. For W/C this was 0.45 and the sand ratio was 40%. Referring to Table 4, five groups of mixes were prepared by using a different percentage of ceramic (0%, 30%, 50%, 70%, and 100%); the replacement percent of ceramic was based on volume. RAC0 was the reference group. Using 100% recycled fine aggregate in the test, the mix proportion is given in Table 4. The water absorption of natural aggregate is lower than that of ceramic aggregate and recycled aggregate, and water absorption is an important indicator that affects the workability and strength of concrete. Higher water absorption of aggregate means more mixing water absorption by the aggregate. Prewetting treatment was adopted for ceramic recycled concrete to ensure consistent water cement ratio, but the prewetting method caused high local water–cement ratio in the interface transition zone, resulting in lower cementite strength in the interface transition zone [47,48]. The greater the water absorption of the aggregate, the more loose its internal structure, and the weaker the bond strength of the transition zone with the cement–mortar interface.

Table 4. Mix proportions.

Item	γ/%	W/C	Materials per Volume (kg/m^3)				
			Water	Cement	Sand	Ceramic	Aggregate
RAC0	0	0.45	180	400	584	0	845
RAC30	30	0.45	180	400	614	102	564
RAC50	50	0.45	180	400	643	170	422
RAC70	70	0.45	180	400	615	260	276
RAC100	100	0.45	180	400	760	402	0

Note: γ represents the replacement ratio of ceramic.

(3) Specimen and test procedure

Mechanical and thermal properties of ceramic concrete were tested according to "Standard for test method of mechanical properties on ordinary concrete" (GB/T 50081-2002) [49] and "Thermal Insulation-Determination of steady-state thermal resistance and related properties-Heat flow meter apparatus" (GB/T 10295-2008) [50]. Cubes of 150 mm were cast to perform the mechanical properties of designed ceramic concrete; 300 mm × 300 mm × 30 mm insulation board was prepared to test the thermal properties, and 390 mm × 190 mm × 190 mm hollow blocks were used to test the mechanical and thermal properties of concrete. The shape of the specimens are shown in Figure 2.

Thermal properties of ceramic concrete board were determined by using a conductometer (JW-III) (Figure 3). After drying and cooling, the board was covered with plastic wrap to prevent contact with surrounding air, and then was placed between the cold and hot plates on the instrument for testing; the hot plate temperature was set to 35 °C and the cold plate temperature was set to 15 °C. The thermal conductivity and thermal inertia index (D) of hollow blocks were calculated according to "Thermal design code for civil building" (GB/T 50176-2016) [51].

Figure 2. Test specimens.

Figure 3. Thermal test.

3. Results, Analysis, and Discussion

3.1. Physical and Mechanical Properties

(1) Ceramic recycled concrete

The replacement ratio of ceramic has a great influence on the density and strength of concrete. The properties of ceramic recycled concrete at different replacement ratios of ceramic aggregate are shown in Figure 4.

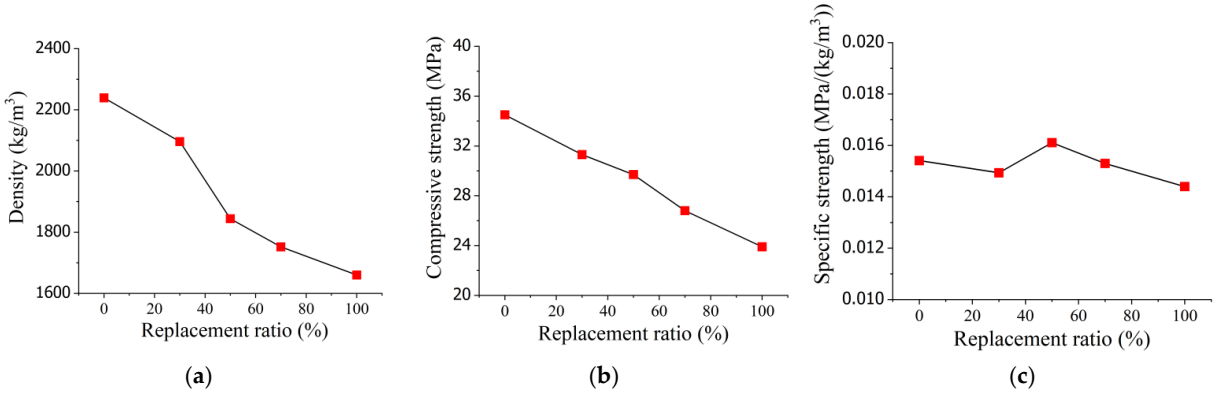

Figure 4. Density and strength of ceramic concrete. (**a**) Density. (**b**) Strength. (**c**) Specific strength.

The apparent density and compressive strength are related properties that are both affected by the replaced ceramic aggregate with different substitution rates. Observing the results of apparent density, it can be seen that the density of ceramic concrete is smaller than that of natural concrete, and the value is decreasing with the increasing replacement ratio of ceramic aggregate. The density is less than 1950 kg/m^3 with a ceramic replacement

ratio higher than 50%, while the density of concrete is reduced 25.8% when the ceramic replacement ratio is up to 100%.

The compressive strength of the concrete is basically between 24 MPa and 34 Mpa, and the strength value is decreasing with the increased replacement ratio of ceramic aggregate. Compared with the 0% ceramic concrete, the compressive strength of ceramic aggregate concrete decreases by 13.9% with 50% ceramic, and when the content of ceramic reaches 100%, its compressive strength decreases by 30.7%. The reduction in the strength mainly depends on the strength of the ceramic, as the interfacial bonding has little effect on strength because of the porosity and roughness character of ceramic.

Density of the ceramic recycled concrete is closely related to its compressive strength; the smaller the density, the lower the compressive strength. Low density of concrete indicates high porosity, meaning its internal structure is relatively looser. The hardness of concrete is also poor, and the bond strength of the transition zone of the cement mortar interface is weak, meaning it is easy to form stress concentrations at the weak point when damaged by pressure, resulting in reduced concrete strength [48]. The damage of the concrete materials is inextricably linked to the interface transition zone. Ensuring the water absorption rate of the aggregate to meet the appropriate water–cement ratio is essential for the design of ceramic recycled concrete strength. Figure 4c shows the specific strength of ceramic concrete. It can be seen that the highest value of specific strength occurs at 50% substitution rate, the density is less than 1950 kg/m^3, and the compressive strength is higher than 30 Mpa. Therefore, the ceramic recycled concrete with a replacement ratio of 50% can be lightweight while ensuring the strength.

(2) Hollow block of ceramic recycled concrete

The replacement ratio of ceramic also has an effect on hollow blocks of ceramic concrete. The physical and mechanical properties at different replacement ratios of ceramic aggregate are shown in Figure 5.

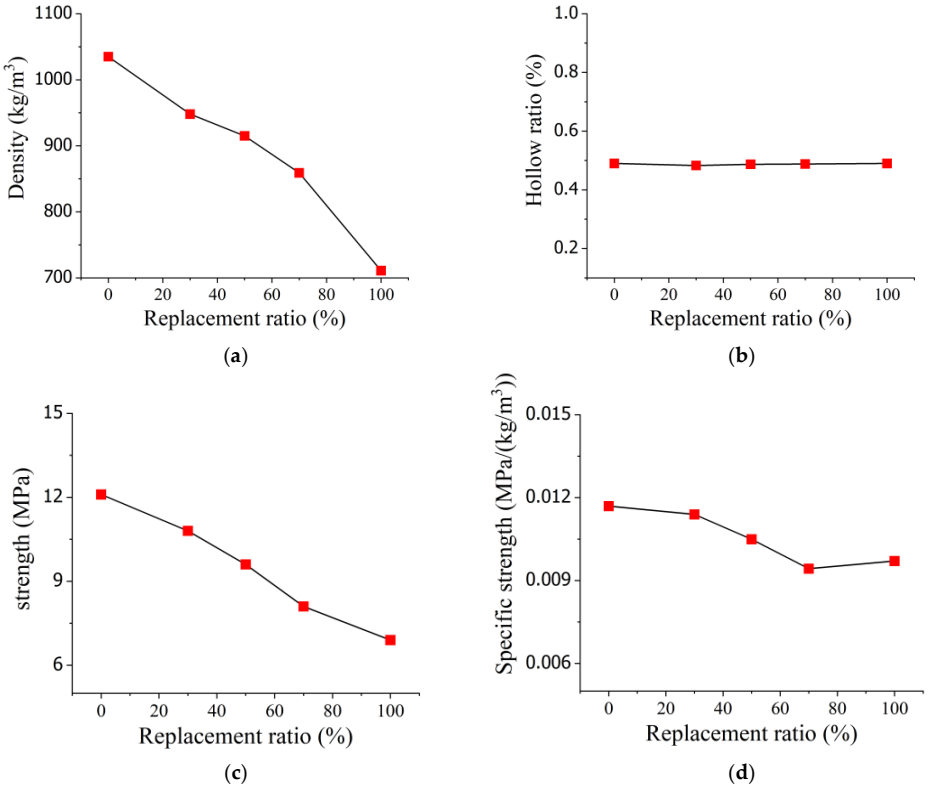

Figure 5. Density and strength of hollow blocks of ceramic concrete. (**a**) Density. (**b**) Hollow ratio. (**c**) Strength. (**d**) Specific strength.

The hollow ratio of the five groups is about 50%, the density is decreasing with the increasing replacement ratio of ceramic aggregate, the value is between 700–1100 kg/m^3 with the ceramic ratio ranging from 0% to 100%. The density of concrete is reduced by 31.2% when the ceramic replacement ratio is up to 100%.

Similar to the compressive strength of ceramic recycled concrete, the strength of hollow blocks of ceramic recycled concrete also decreases with the increased replacement ratio of ceramic aggregate. Compared with the 0% ceramic concrete, the compressive strength of ceramic aggregate concrete decreases by 20% with 50% ceramic and 42.5% with 100%, and the magnitude of decrease in compressive strength is slightly greater in hollow block concrete than in ceramic concrete. Figure 5d shows the specific strength of hollow block ceramic concrete. It can be seen that value is higher than 0.01 with the replacement ratio of ceramic of less than 50%, which indicates that the utilization of ceramic should be controlled to ensure the strength of the hollow blocks.

3.2. Thermal Conductivity of Concrete Insulation Board

Table 5 shows the thermal conductivity of the insulation boards made with ceramic and recycled aggregate. The subsequent use of ceramic aggregate leads to a drop in thermal conductivity of concrete with different replacement ratios. As the average thermal conductivity with replacement ratio of ceramic increases from 0% to 100%, it correspondingly decreases from 1.457 W/(m·K) to 0.192 W/(m·K). Observing the results of thermal conductivity, it can be seen that the average value of ceramic recycled concrete with 100% substitution rate is only about 1/7 of that of the concrete with a 0% substitution rate. Conversely, the thermal resistance increases when the ceramic replacement ratio increases, with the average value changing from 0.021 m^2·K/W to 0.154 m^2·K/W. The smaller the thermal conductivity, the better the thermal insulation performance, which indicates that ceramic recycled concrete has an excellent thermal insulation performance.

Table 5. Thermal conductivity of insulation board.

Specimen	Thermal Conductivity (W/(m·K)	Average(W/(m·K)	Thermal Resistance(m^2·K/W)	Average (m^2·K/W)
RC-0-1	1.465	1.457	0.021	0.021
RC-0-2	1.441		0.021	
RC-0-3	1.465		0.021	
RC-30-1	0.498	0.503	0.060	0.059
RC-30-2	0.512		0.058	
RC-30-3	0.501		0.059	
RC-50-1	0.308	0.301	0.098	0.100
RC-50-2	0.297		0.101	
RC-50-3	0.295		0.101	
RC-70-1	0.254	0.246	0.117	0.121
RC-70-2	0.235		0.126	
RC-70-3	0.249		0.121	
RC-100-1	0.190	0.192	0.153	0.154
RC-100-2	0.194		0.155	
RC-100-3	0.192		0.154	

The density of ceramic recycled concrete is related to its thermal conductivity. The physical and thermal properties are both affected by the ceramic replacement ratio, and the correlations of density and thermal property are shown in Figure 6. The results show that the thermal conductivity follows a similar trend to the density, as with the ceramic replacement ratio varying from 0% to 100%, the thermal conductivity and thermal resistance have the opposite trend. Density, strength, and thermal conductivity are interrelated. The smaller the density, the lower the thermal conductivity, and in such a case, concrete has

good thermal insulation; but the smaller the density, the lower the concrete strength. The use of ceramic demonstrates an opposite effect on the mechanical properties of concrete. The test shows that a 50% replacement ratio of ceramic aggregate is appropriate combined with thermal and mechanical requirements.

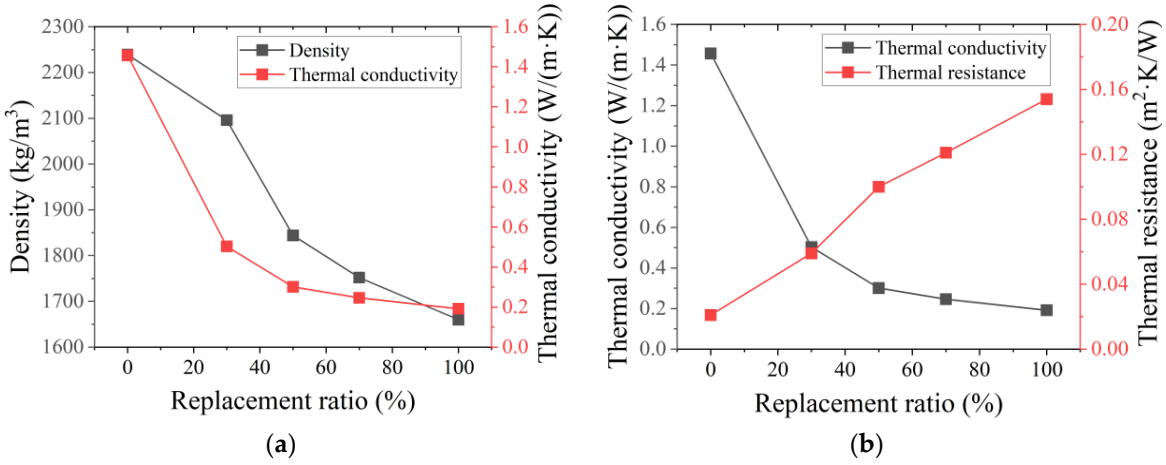

Figure 6. Thermal conductivity of concrete insulation board. (**a**) Density and thermal conductivity. (**b**) Thermal conductivity and thermal resistance.

3.3. Thermal Conductivity of Concrete Hollow Blocks

1. Heat conductivity

The thermal resistance of envelope structure can be calculated as follows:

(1) For single layer structure:

$$R = \frac{\delta}{\lambda} \tag{5}$$

In which δ represents the thickness of structure, and λ represents the thermal conductivity of material.

(2) For multilayer structure:

$$R = \sum R_j \tag{6}$$

In which R_j represents the thermal resistance of each layer of material.

The division of heat transfer channels is shown in Figure 7; they are divided into five channels parallel to the heat transfer direction.

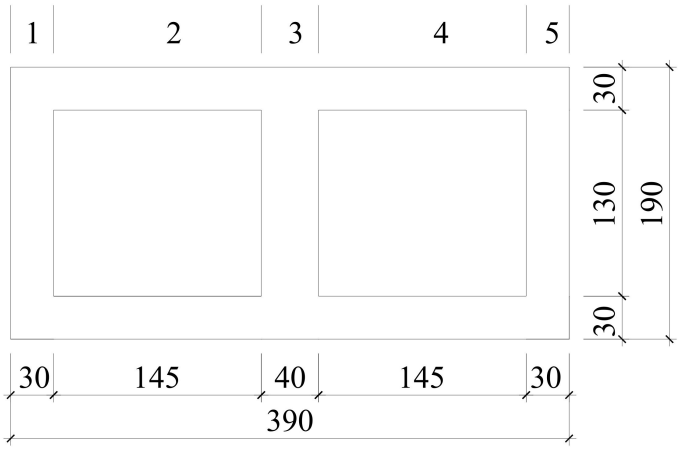

Figure 7. Heat transfer channel.

(3) Average thermal resistance of multilayer heterogeneous structure:

$$\overline{R} = \left[\frac{F_0}{\frac{F_1}{R_{01}} + \frac{F_2}{R_{02}} + \ldots + \frac{F_N}{R_{0n}}} - (R_i + R_e) \right] \varphi \quad (7)$$

In which F_0 represents the total heat transfer area, F_n represents each heat transfer area, R_{0n} represents thermal resistance of each heat transfer surface, and φ represents the correction coefficient.

The thermal resistance of each channel can be calculated based on Formula (5) and Formula (6), and then the average value can be determined according to Formula (7). The calculated result is shown in Table 6.

Table 6. Average thermal resistance.

Item	Channel-1 (m^2·K/W)	Channel-2 (m^2·K/W)	Channel-3 (m^2·K/W)	Channel-4 (m^2·K/W)	Channel-5 (m^2·K/W)	φ	$\overline{R}$ (m^2·K/W)
RC-0	0.280	0.371	0.280	0.371	0.280	0.93	0.179
RC-30	0.528	0.449	0.528	0.449	0.528	0.93	0.295
RC-50	0.781	0.529	0.781	0.529	0.781	0.96	0.410
RC-70	0.922	0.574	0.922	0.574	0.922	0.98	0.476
RC-100	1.140	0.643	1.140	0.643	1.140	0.98	0.562

Total thermal resistance can be calculated as:

$$R_0 = R_i + \overline{R} + R_e \quad (8)$$

In which R_i represents the internal surface heat exchange resistance, and R_e represents the external surface heat exchange resistance.

Heat conductivity can be calculated as:

$$K = \frac{1}{R_0} \quad (9)$$

The thermal resistance and heat conductivity can be calculated, and the result is shown in Table 7. The thermal resistance increases when the ceramic replacement ratio increases, with the value increasing from 0.374 m^2·K/W to 0.756 m^2·K/W. Similar to the ceramic concrete board, the use of ceramic aggregate leads to a drop in the thermal conductivity of concrete: the value decreases from 2.676 W/(m·K) to 1.322 W/(m·K) when the ceramic ratio increases from 0% to 100%. It indicates that the thermal insulation performance of hollow block concrete is improved with the use of ceramic.

Table 7. Thermal resistance and heat conductivity.

Item	R(m^2·K/W)	K (W/(m·K))
RC-0	0.374	2.676
RC-30	0.489	2.043
RC-50	0.604	1.654
RC-70	0.670	1.492
RC-100	0.756	1.322

2. Thermal inertia index

The thermal inertia index of envelope structure can be calculated as follows:

(1) For single layer structure:

$$D = RS \quad (10)$$

In which R represents the thermal resistance, and S represents the thermal storage coefficient of material. The equation of S can be expressed as:

$$S = \sqrt{\frac{2\pi cp\lambda}{T}} \tag{11}$$

In which c represents the heat capacity, ρ represents the apparent density, λ represents the thermal conductivity of material, and T represents 24 h.

(2) For multilayer structure:

$$D = \sum D_n \tag{12}$$

In which D_n represents the thermal inertia index of each layer of material.

The heat insulation channels are divided as shown in Figure 8; they are divided into three channels parallel to the heat insulation direction.

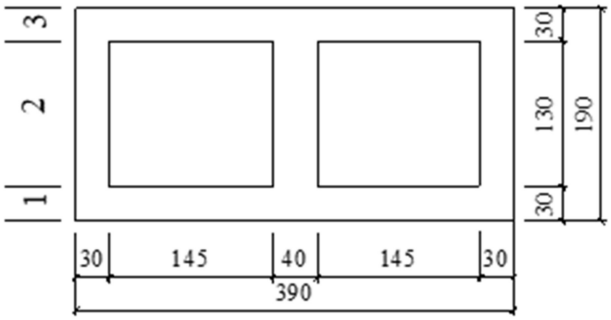

Figure 8. Heat insulation channel.

(3) Average thermal inertia index of multilayer heterogeneous structure

$$\overline{D} = \overline{RS} \tag{13}$$

In which $\overline{R}$ represents the average thermal resistance and $\overline{S}$ represents the average thermal storage coefficient. $\overline{R}$ and $\overline{S}$ can be expressed as:

$$\overline{R} = \frac{\delta}{\left(\frac{\lambda_1 F_{1+}\lambda_2 F_{2+}\ldots\lambda_n F_n}{F_{1+}F_{2+}\cdots F_n}\right)} \tag{14}$$

$$\overline{S} = \frac{S_1 F_{1+} S_2 F_{2+}\ldots S_n F_n}{F_{1+}F_{2+}\cdots F_n} \tag{15}$$

According to Formulas (10)–(15), the average thermal resistance and thermal storage coefficient can be calculated, and the average thermal inertia index is calculated and shown in Table 8.

Table 8. Average thermal inertia index.

Item	$\overline{R}$ (m^2·K/W)			$\overline{S}$ (W/(m^2·K))			$\overline{D}$
	Channel-1	Channel-2	Channel-3	Channel-1	Channel-2	Channel-3	
RC-0	0.02	0.15	0.02	19.96	5.12	19.96	1.58
RC-30	0.06	0.39	0.06	16.48	4.23	16.48	3.60
RC-50	0.10	0.59	0.10	12.28	3.15	12.28	4.30
RC-70	0.12	0.68	0.12	10.99	2.82	10.99	4.61
RC-100	0.16	0.82	0.16	9.23	2.37	9.23	4.81

The final heat conductivity and thermal inertia index is shown in Table 9 with considering the plaster factor. The heat conductivity decreases when the ceramic replacement ratio increases, and thermal inertia index D is increases with the ceramic added.

Table 9. Heat conductivity and thermal inertia index.

Item	K (W/(m·K))	*D*
RC-0	2.676	2.07
RC-30	2.043	4.09
RC-50	1.654	4.79
RC-70	1.492	5.10
RC-100	1.322	5.30

Density is related to thermal conductivity and thermal inertia index. The interrelationship of the physical and thermal properties of ceramic hollow blocks is shown in Figure 9. The results show that with the increasing replacement rate of ceramic, the heat conductivity of hollow blocks decreases in turn, and the thermal inertia index D increases. Lower heat conductivity matches the greater thermal inertia index, which demonstrates that the hollow blocks have a better insulation performance with ceramic added. Therefore, on the premise of ensuring the mechanical properties of hollow blocks, the proper addition of ceramic aggregate can effectively improve the thermal insulation performance of concrete. Figure 9c shows the comparison from different works in the literature. With different additives in concrete, the thermal properties of concrete vary greatly, but the main trends are similar: the thermal conductivity increases with the increase in density. The ceramic concrete in this study has a faster growth rate, mainly due to the high porosity made by the combined use of ceramic coarse aggregate and recycled fine aggregate.

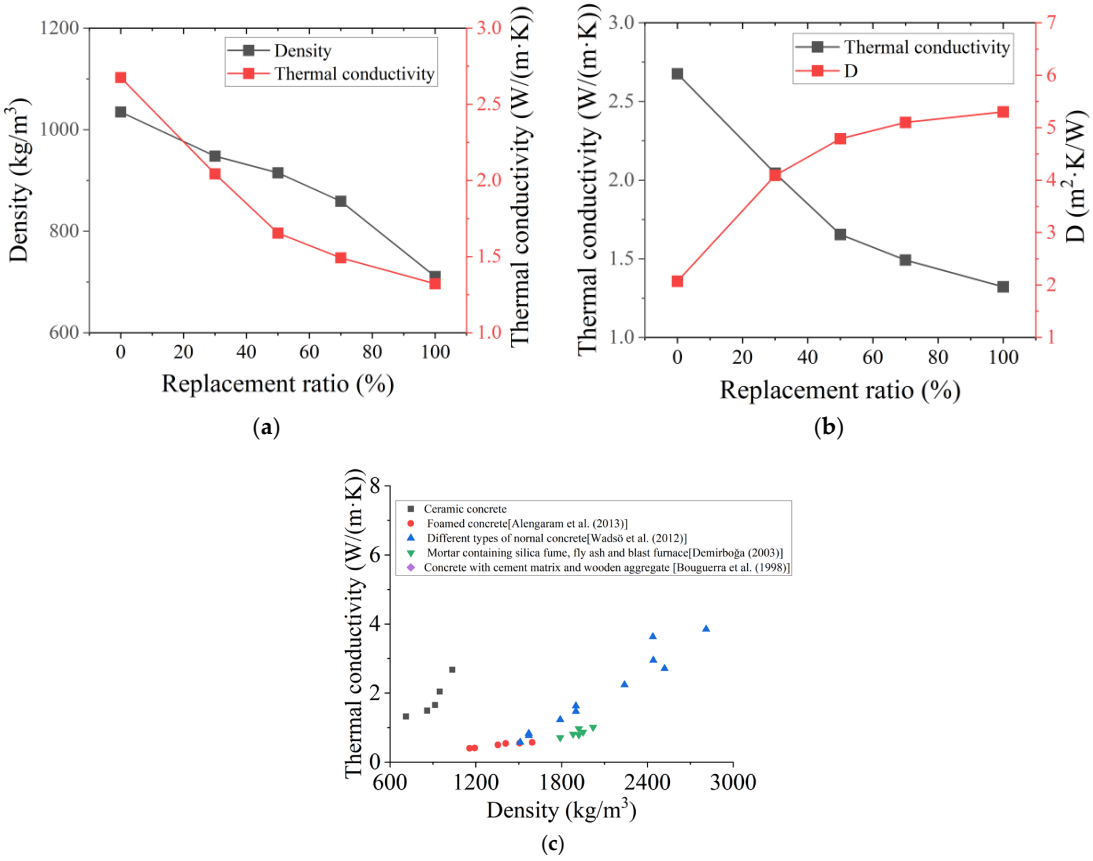

Figure 9. Thermal conductivity of concrete hollow block. (**a**) Density and thermal conductivity. (**b**) Thermal conductivity and D. (**c**) Comparison with data from the literature [52–55].

4. Conclusions

Based on the results and the analysis, some conclusions can be drawn:

1. The density and strength of ceramic recycled concrete are directly related, and both are affected by ceramic aggregate replacement ratio. Properly adjusting the amount of ceramic aggregate can meet the different requirements for concrete strength;
2. For ceramic recycled concrete board, the physical property is directly related to its thermal properties: the smaller the density, the lower the thermal conductivity and higher thermal resistance. The addition of ceramic aggregate can improve the thermal insulation performance of concrete;
3. For ceramic hollow blocks, the variation in thermal performance with ceramic aggregate content is similar to that of ceramic recycled concrete: with the increase in ceramic aggregate ratio, the thermal conductivity decreases and the thermal inertia index D increases. The amount of ceramic aggregate should be seriously considered to balance the relationship between mechanical properties and thermal properties;
4. The use of ceramic recycled concrete as a non-load-bearing construction material can overcome its disadvantages in mechanical properties and fully reflect its functional advantages, with good environmental and economic benefits.

Author Contributions: Conceptualization, Y.W. and J.W.; methodology, Y.W.; validation, Y.W., J.W. and Z.D.; formal analysis, Y.W. and J.X.; resources, Z.D. and J.X.; data curation, J.W.; writing—original draft preparation, Y.W.; writing—review and editing, J.W. and J.X.; supervision, Z.D. and J.X.; funding acquisition, J.X. and Z.D. All authors have read and agreed to the published version of the manuscript.

Funding: This work is supported by the National Natural Science Foundation of China (grants no. 51661145023 and no. 51868005).

Institutional Review Board Statement: Not applicable.

Informed Consent Statement: Not applicable.

Data Availability Statement: No new data were created.

Conflicts of Interest: The authors declare no conflict of interest.

References

1. Xiao, J. *Recycled Aggregate Concrete Structures*; Springer: Berlin/Heidelberg, Germany, 2018; ISBN 9783662539859.
2. Rezaei, S.D.; Shannigrahi, S.; Ramakrishna, S. A review of conventional, advanced, and smart glazing technologies and materials for improving indoor environment. *Sol. Energy Mater. Sol. Cells* **2017**, *159*, 26–51. [CrossRef]
3. Deba, C.; Zhang, F.; Yang, J.; Lee, S.E.; Shah, K.W. A review on time series forecasting techniques for building energy consumption. *Renew. Sustain. Energy Rev.* **2017**, *74*, 902–924. [CrossRef]
4. Shen, L.Y.; Tam, V.W.; Tam, C.M.; Drew, D. Mapping approach for examining waste management on construction sites. *J. Constr. Eng. Manag.* **2004**, *130*, 472–481. [CrossRef]
5. Ginga, C.P.; Ongpeng, J.M.C.; Daly, M.; Klarissa, M. Circular economy on construction and demolition waste: A literature review on material recovery and production. *Materials* **2020**, *13*, 2970. [CrossRef]
6. Forward. *Report of Market Research and Investment Forecast Analysis on China Construction and Demolition Waste Disposal Industry (2020–2025)*; Forward Business Information Co. Ltd.: Shenzhen, China, 2020.
7. Prakash, R.; Raman, S.N.; Subramanian, C.; Divyah, N. 6—Eco-friendly fiber-reinforced concretes. In *Handbook of Sustainable Concrete and Industrial Waste Management*; Woodhead Publishing: Cambridge, UK, 2022; pp. 109–145. [CrossRef]
8. Prakash, R.; Divyah, N.; Srividhya, S.; Avudaiappan, S.; Amran, M.; Raman, S.N.; Guindos, P.; Vatin, N.I.; Fediuk, R. Effect of Steel Fiber on the Strength and Flexural Characteristics of Coconut Shell Concrete Partially Blended with Fly Ash. *Materials* **2022**, *15*, 4272. [CrossRef]
9. Prakash, R.; Thenmozhi, R.; Raman, S.N.; Subramanian, C. Characterization of eco-friendly steel fiber-reinforced concrete containing waste coconut shell as coarse aggregates and fly ash as partial cement replacement. *Struct. Concr.* **2020**, *21*, 437–447. [CrossRef]
10. Wu, H.; Zuo, J.; Zillante, G.; Wang, J.; Yuan, H. Construction and demolition waste research: A bibliometric analysis. *Archit. Sci. Rev.* **2019**, *62*, 354–365. [CrossRef]
11. Fonseca, F.L.C.; Namen, A.A. Characteristics and patterns of inappropriate disposal of construction and demolition waste in the municipality of Cabo Frio, Brazil. *Urbe. Rev. Bras. Gestão Urbana* **2021**, *13*, e20200091. [CrossRef]

12. Posi, P.; Thongjapo, P.; Thamultree, N.; Boontee, P.; Kasemsiri, P.; Chindaprasirt, P. Pressed lightweight fly ash-OPC geopolymer concrete containing recycled lightweight concrete aggregate. *Constr. Build. Mater.* **2016**, *127*, 450–456. [CrossRef]
13. Pham, T.M.; Elchalakani, M.; Hao, H.; Lai, J.; Ameduri, S.; Tran, T.M. Durability characteristics of lightweight rubberized concrete. *Constr. Build. Mater.* **2019**, *224*, 584–599. [CrossRef]
14. Divyah, N.; Prakash, R.; Srividhya, S.; Sivakumar, A. Parametric study on lightweight concrete-encased short columns under axial compression-Comparison of design codes. *Struct. Eng. Mech.* **2022**, *83*, 387–400. [CrossRef]
15. Prakash, R.; Raman, S.N.; Divyah, N.; Subramanian, C.; Vijayaprabha, C.; Praveenkumar, S. Fresh and mechanical characteristics of roselle fibre reinforced self-compacting concrete incorporating fly ash and metakaolin. *Constr. Build. Mater.* **2021**, *290*, 123209. [CrossRef]
16. Xie, J.; Zhao, J.; Wang, J.; Huang, P.; Liu, J. Investigation of the high-temperature resistance of sludge ceramsite concrete with recycled fine aggregates and GGBS and its application in hollow blocks. *J. Build. Eng.* **2021**, *34*, 101954. [CrossRef]
17. Zhai, X.; Yan, J.; Cao, C. Seismic performance and flexible connection optimization of prefabricated integrated short-leg shear wall filled with ceramsite concrete. *Constr. Build. Mater.* **2021**, *311*, 125224. [CrossRef]
18. Shen, Y.; Huang, J.; Ma, X.; Hao, F.; Lv, J. Experimental study on the free shrinkage of lightweight polymer concrete incorporating waste rubber powder and ceramsite. *Compos. Struct.* **2020**, *242*, 112152. [CrossRef]
19. Rathore, P.K.S.; Gupta, N.K.; Yadav, D.; Shu, K.; Kaul, S. Thermal performance of the building envelope integrated with phase change material for thermal energy storage: An updated review. *Sustain. Cities Soc.* **2022**, *79*, 103690. [CrossRef]
20. Fan, L.D.; Zhang, Z.J.; Yu, Y.Q.; Li, P.T.; Cosgrove, T. Effect of elevated curing temperature on ceramsite concrete performance. *Constr. Build. Mater.* **2017**, *153*, 423–429. [CrossRef]
21. Kim, H.K.; Jeon, J.H.; Lee, H.K. Workability, and mechanical, acoustic and thermal properties of lightweight aggregate concrete with a high volume of entrained air. *Constr. Build. Mater.* **2012**, *29*, 193–200. [CrossRef]
22. Han, R.B.; Xu, Z.M.; Qing, Y.T. Study on the Material Performance of Ceramsite Concrete Roof Brick. *Procedia Eng.* **2017**, *205*, 642–649. [CrossRef]
23. Jo, B.W.; Park, S.K.; Jong-bin Park, J.B. Properties of concrete made with alkali-activated fly ash lightweight aggregate (AFLA). *Cem. Concr. Comp.* **2006**, *35*, 1235–1243. [CrossRef]
24. Cheeseman, C.R.; Virdi, G.S. Properties and microstructure of lightweight aggregate produced from sintered sewage sludge ash Resources. *Conserv. Recycl.* **2005**, *45*, 18–30. [CrossRef]
25. Hou, Z.; Tang, J. *Technical Property and Applying for Bridge Deck of Ceramsite Concrete*; American Society of Civil Engineers: Reston, VA, USA, 2011; pp. 1898–1903. [CrossRef]
26. Yuan, H.Q.; Jing, H.; Tang, D.Y.; Liu, W.L. Mechanical properties of shale ceramisite concrete with recycled rubber powder under compression. *J. Build. Mater.* **2007**, *10*, 369–373.
27. Malaiškiene, J.; Vaiciene, M.; Zurauskien, R. Effectiveness of technogenic waste usage in products of building ceramics and expanded clay concrete. *Constr. Build. Mater.* **2011**, *25*, 3869–3877. [CrossRef]
28. Liu, J.Z.; Ba, M.F.; He, Z.M.; Li, Y.S. Microstructure and performance of sludge-ceramisite concrete. *Constr. Build. Mater.* **2013**, *39*, 82–88. [CrossRef]
29. Alessandro, A.; Pisello, A.L.; Fabiani, C.F. Multifunctional smart concretes with novel phase change materials: Mechanical and thermo-energy investigation. *Appl. Energy* **2018**, *212*, 1448–1461. [CrossRef]
30. Ling, T.C.; Poon, C.S. Use of phase change materials for thermal energy storage in concrete: An overview. *Constr. Build. Mater.* **2013**, *46*, 55–62. [CrossRef]
31. Ding, W.H.; Zhu, L.; Li, H.; Hou, B.; Yang, F. Mechanical and Thermal Properties of Shale Ceramsite Concrete: Experimental Study on the Influence Law due to Microencapsulated Phase-Change Material Content and Phase-Change Cycle Numbers. *Adv. Civ. Eng.* **2022**, *2022*, 2720956. [CrossRef]
32. Xiao, J.; Li, W.; Fan, Y.; Huang, X. An overview of study on recycled aggregate concrete in China (1996–2011). *Constr. Build. Mater.* **2012**, *31*, 364–383. [CrossRef]
33. Hamad, B.S.; Dawi, A.H. Sustainable normal and high strength recycled aggregate concretes using crushed tested cylinders as coarse aggregates. *Case Stud. Constr. Mater.* **2017**, *7*, 228–239. [CrossRef]
34. Hansen, T.C. Recycled aggregates and recycled aggregate concrete second state-of-the-art report developments 1945–1985. *Mater. Struct.* **1986**, *19*, 201–246. [CrossRef]
35. Khatib, J.M. Properties of concrete incorporating fine recycled aggregate. *Cem. Concr. Res.* **2005**, *35*, 763–769. [CrossRef]
36. Braga, M.; de Brito, J.; Veiga, R. Incorporation of fine concrete aggregates in mortars. *Constr. Build. Mater.* **2012**, *36*, 960–968. [CrossRef]
37. Kou, S.C.; Poon, C.S. Properties of concrete prepared with crushed fine stone, furnace bottom ash and fine recycled aggregate as fine aggregates. *Constr. Build. Mater.* **2009**, *23*, 2877–2886. [CrossRef]
38. Evangelista, L.; de Brito, J. Mechanical behaviour of concrete made with fine recycled concrete aggregates. *Cem. Concr. Compos.* **2007**, *29*, 397–401. [CrossRef]
39. Etxeberria, M.; Vázquez, E.; Marí, A.; Barra, M. Influence of amount of recycled coarse aggregates and production process on properties of recycled aggregate concrete. *Cem. Concr. Res.* **2007**, *37*, 735–742. [CrossRef]
40. Zhao, Z.F.; Remond, S.; Damidot, D.; Xu, W.Y. Influence of fine recycled concrete aggregates on the properties of mortars. *Constr. Build. Mater.* **2015**, *81*, 179–186. [CrossRef]

41. Li, Z.; Liu, J.P.; Xiao, J.Z.; Zhong, P.H. A method to determine water absorption of recycled fine aggregate in paste for design and quality control of fresh mortar. *Constr. Build. Mater.* **2019**, *197*, 30–41. [CrossRef]
42. *GB/T 17431.2-2010*; Lightweight Aggregates and Its Test Methods—Part 2: Test Methods for Lightweight Aggregates. National Standards of the People's Republic of China: Beijing, China, 2010.
43. *GB/T 14685-2011*; Pebble and Crushed Stone for Construction. National Standards of the People's Republic of China: Beijing, China, 2011.
44. *GB/T 25176-2010*; Recycled Fine Aggregate for Concrete and Mortar. National Standards of the People's Republic of China: Beijing, China, 2010.
45. *JGJ51-2002*; Technical Specification for Lightweight Aggregate Concrete. Industry standard of the People's Republic of China: Beijing, China, 2002.
46. *DG/TJ08-2018-2007*; Technical Code on the Application of Recycled Concrete. Shanghai Engineering Construction Code: Shanghai, China, 2007.
47. Sagoe-Crentsil, K.K.; Brown, T.; Taylar, A.H. Performance of concrete made with commercially produced coarse recycled concrete aggregate. *Cem. Concr. Res.* **2001**, *31*, 707–712. [CrossRef]
48. Xiao, J.Z.; Liu, Q.; Du, J.T.; Zhang, C.Z. Micro-damage mechanisms and property fluctuation off recycled aggregate concrete. *Key Eng. Mater.* **2007**, *348*, 611–664. [CrossRef]
49. *GB/T 50081-2002*; Standard for Test Method of Mechanical Properties on Ordinary Concrete. National Standards of the People's Republic of China: Beijing, China, 2002.
50. *GB/T 10295-2008*; Thermal Insulation-Determination of Steady-State Thermal Resistance and Related Properties—Heat Flow Meter Apparatus. National Standards of the People's Republic of China: Beijing, China, 2008.
51. *GB 50176-2016*; Code for Thermal Design of Civil Building. National Standards of the People's Republic of China: Beijing, China, 2016.
52. Alengaram, U.J.; Al Muhit, B.A.; bin Jumaat, M.Z.; Jing, M.L.Y. A comparison of the thermal conductivity of oil palm shell foamed concrete with conventional materials. *Mater. Design* **2013**, *51*, 522–529. [CrossRef]
53. Wadsö, L.; Karlsson, J.; Tammo, K. Thermal properties of concrete with various aggregates. Engineering. 2012. Available online: http://www.byggnadsmaterial.lth.se/fileadmin/byggnadsmaterial/Research/CERBOF/Thermal_properties__nr_10_.pdf (accessed on 23 October 2022).
54. Demirboğa, R. Influence of mineral admixtures on thermal conductivity and compressive strength of mortar. *Energy Build.* **2003**, *35*, 189–192. [CrossRef]
55. Bouguerra, A.; Ledhem, A.; De Barquin, F.; Dheilly, R.; Queneudec, M. Effect of microstructure on the mechanical and thermal properties of lightweight concrete prepared from clay, cement, and wood aggregates. *Cem. Concr. Res.* **1998**, *28*, 1179–1190. [CrossRef]